Modeling of potential distribution of subsea pipeline under cathodic protection by finite element method

P. Marcassoli*, A. Bonetti, L. Lazzari and M. Ormellese

(Received: April 2, 2014)
(Accepted: April 28, 2014)

1 Introduction

The use of cathodic protection (CP) on offshore platforms and pipelines, if properly applied, represents a cost effective solution to ensure their integrity against severe external corrosion produced by an aggressive environment such as seawater. Years of experience gathered by oil and gas companies and scientific community have developed a strong and sound CP engineering, based on the use of both galvanic anodes and impressed current systems [1].

However, CP has to be periodically monitored in order to verify anode consumption or current output and check proper protection condition, through potential measurement, to prevent either lack of protection or overprotection.

Subsea pipelines are often protected by a combination of an external coating and galvanic anodes, generally as bracelet and, less frequently, as sled. Due to the relatively low ohmic drop in seawater, throwing power of CP is high, then allowing a high anode spacing.

Survey activities on offshore pipelines are carried out by a ROV (remotely operated vehicle), which permits the visual assessment and the measurements of the protection potential and the current density. For this purpose, a tailored probe, mounted on the ROV, is used, which enables the measurement and recording of the potential profile and the local ohmic drop along the pipeline.

The potential is measured against a reference electrode, embedded in the probe, whilst the local ohmic drop is measured by means of two reference electrodes assembled at a fixed distance on the probe. The local ohmic drop profile (or the current density profile) along the pipeline shows peaks, with opposite direction, in correspondence of coating defects and anodes. As far as defects are concerned, it is not immediate to establish whether CP is sufficient and to estimate their size, since current and potential distributions are unknown; furthermore, the knowledge of the size is important in order to make a decision about the need of a repair.

The solution of this problem is the finite element method (FEM) analysis [2–5]. The use of simulations and modeling is nowadays suggested also by standards such as Norsok M-503 to study complex systems and assist traditional engineering approach [6]. By applying FEM analysis, the electrical field is solved so that current and potential distribution in every point of the pipeline are gained [7].

P. Marcassoli, A. Bonetti
Cescor srl, 12, Via Maniago 20134, Milan, (Italy)
E-mail: paolo.marcassoli@cescor.it

L. Lazzari, M. Ormellese
Politecnico di Milano, Dip. CMIC "G. Natta", 7, Via Mancinelli 20134, Milan, (Italy)

In this work, a simplified 2-dimensional model was used for a coated pipeline protected with bracelet anodes; as first approximation, the coating was assumed as a perfect insulator and some defects with different sizes were considered present. Other parameters such as sea depth and burial depth were varied to evaluate their effect. By overlapping field data and FEM simulation results, a relationship between measured IR drop and the defect size was obtained, as well as the minimum detectable defect size by the method. This approach provides a meaningful interpretation of CP conditions within the activities for the pipeline integrity assessment.

2 Model

2.1 Model domain

For solving the electrical field near coating damages of an offshore pipeline under CP, a two-dimensional, 2D, model was considered. The model domain is schematically shown in Fig. 1. A section of a 300 m long pipeline was represented with a one-dimensional element, in which a galvanic bracelet anode (0.5 m long) is positioned at the center. The coating of the pipe has one or more defects of size w, located at a distance x_n from the center of the anode. The mud layer covering the pipeline (where present) and seawater depth are designated h_m and h_s, respectively.

2.2 Physical properties

As far as the properties of the 2D domain adopted for finite element analysis are concerned, in order to solve the electrical field, the following resistivity values were used:

- Seawater resistivity $\rho_s = 0.2\,\Omega\,m$ (conductivity of 5 S/m)
- Mud resistivity $\rho_m = 1.0\,\Omega\,m$ (conductivity of 1 S/m)

2.3 Geometrical parameters

Five values of sea depth, h_s, were considered: 5, 10, 30, 100, and 300 m.

Four values of burial depth, h_m, were studied: 0.5, 1, 1.5, and 2 m. Simulations were also performed in the case of h_m zero, i.e. pipeline laid on sea bottom (i.e. not buried).

The position of the defects on the domain axis was defined symmetrically with the center of the anode: accordingly, two distances were considered, namely 75 and 150 m for a single coating defect case study, and at −150, −75, 75, and 150 m for the case study of four coating defects.

In all cases the length of the bracelet anode was 0.5 m.

The complete screening of FEM calculations was based on a coating defect size of 10 mm; to evaluate the influence of the defect size on the ohmic drop and the electrical field close to the damage, the values of 1, 20, 50, and 100 mm were also taken into account.

2.4 Electrochemical parameters and boundary conditions

The boundary conditions considered for solving the electric field were the following:

- Anode potential constant and equal to −1.1 V SCE
- Perfect insulation capability of the coating
- Electrical insulation at the free surface of the sea and at the lateral edges of the domain
- Potential and current density in correspondence of the coating defect defined by the Butler–Volmer equation: [1]

$$i = i_{corr} \cdot e^{-2.303(E-E_{corr})/b_a} - i_L - i_{H_2} \cdot e^{-2.303(E-E_{H_2})/b_{H_2}} \quad (1)$$

where the first term is the anodic curve, the second one represents the oxygen limiting current density and the third is the curve related with hydrogen evolution by water dissociation.

$$2H_2O + 2e^- \rightarrow H_2 \uparrow + 2\,OH^- \quad (2)$$

The contribution by the cathodic reaction of reduction of hydrogen ion is negligible at pH values near neutral or alkaline.

$$2H^+ + 2e^- \rightarrow H_2 \uparrow \quad (3)$$

The values of the parameters in Equation (1) are as follow:

- $i_{corr} = i_L$ due to the oxygen reduction as dominant cathodic process (corrosion current density)
- $b_a = 60$ mV/dec (anodic Tafel slope)
- $i_L = 50\,mA/m^2$ if pipeline not buried; $i_L = 15\,mA/m^2$ if buried pipeline (i_L is the oxygen limiting current density)

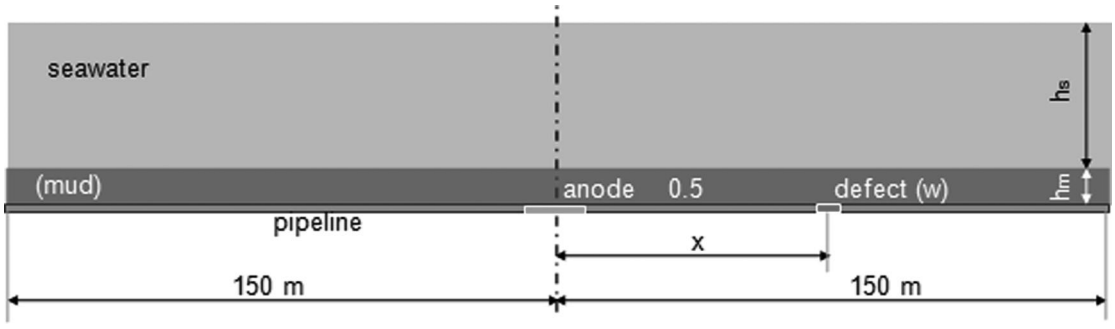

Figure 1. Model domain and parameters

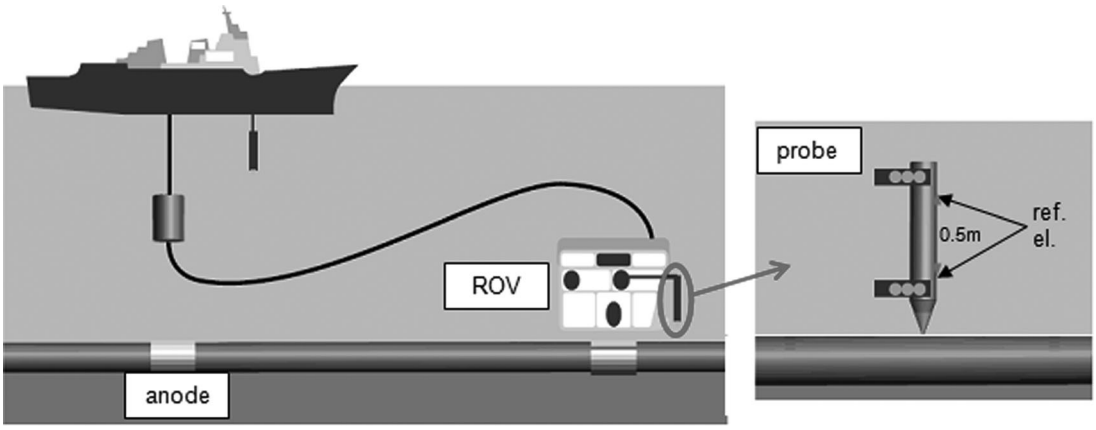

Figure 2. ROV and CP probe scheme

- $i_{H_2} = 0.02\ \text{mA/m}^2$ (hydrogen exchange current density on steel)
- $E_{H_2} = -0.7\ \text{V}$ *versus* SCE (hydrogen equilibrium potential)
- $b_{H_2} = 120\ \text{mV/dec}$ (hydrogen Tafel slope)

2.5 Remotely operated vehicle (ROV)

FEM results were compared with a real monitoring performed with a dedicated ROV equipped with two Ag/AgCl reference electrodes mounted at a fixed distance (0.5 m) on a CP probe. Figure 2 shows a schematic representation of the ROV and the CP probe.

During surveys, the ROV moves along the pipeline at a fixed distance, keeping the tip of the probe at about 0.2 m from the pipeline; consequently the two reference electrodes mounted on the probe are at 0.3 and 0.8 m from the metallic surface or from the mud surface, if the pipeline is buried.

The minimum local ohmic drop detectable by this measurement system is 0.1 mV.

3 FEM calculations

The numerical solving of the electric field in the domain was performed using the commercial software COMSOL Multiphysics® v3.5*. The geometry of the domain, its properties and boundary conditions were defined and set on the basis of the values given in the previous paragraph. The 2D domain was discretized by means of triangular shaped elements.

The mesh was first initialized, then refined with one or more automated steps and further thickened in correspondence with those "segments" representing the anode and the coating defect; typically, elements of approximately an order of magnitude smaller than the size of the segments (typically eight elements or a higher number per segment) were used, for a the total number in the domain of the order of 10^6. In the case of buried pipeline, the mud sub-domain mesh was refined by fixing maximum element dimension.

The electric field was obtained by two solving steps:

- calculation of the primary current distribution, i.e. distribution related to ohmic drops only, setting a potential of −0.6 V *versus* SCE at the defect surface;
- calculation of the secondary current distribution, i.e. electric field related with electrochemical processes and their overpotentials, by setting the boundary condition in Equation (1).

At the end of each simulation the integral values of current at the anode and cathode were compared to verify the consistency of the results. The potential *versus* current density plot was compared with the characteristic curves defined by boundary conditions (Fig. 3). All values were coherent with the boundary condition in Equation (1).

3.1 Single defect *versus* four equally spaced defects

Figure 4 shows the potential distribution obtained for a single coating defect (a, b) located at 75 and 150 m from the anode, respectively, and the one obtained for four equally spaced defects (c). Figure 5 shows the potentials obtained for different sea depths for same configurations in the case of pipeline laid on sea bottom. It appears that the presence of multiple defects determines a significant change in the distribution of the potential and the current in the domain.

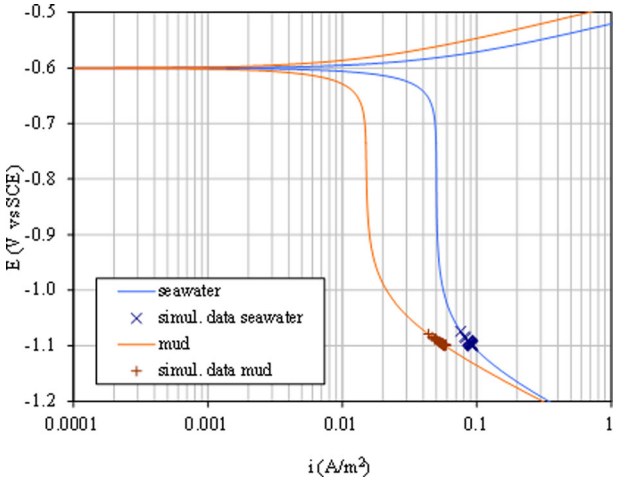

Figure 3. Comparison between the values of potential and current density at the anode obtained by FEM analysis and the characteristic curves derived from Equation (1) in the case of the absence and presence of a mud layer above the pipeline

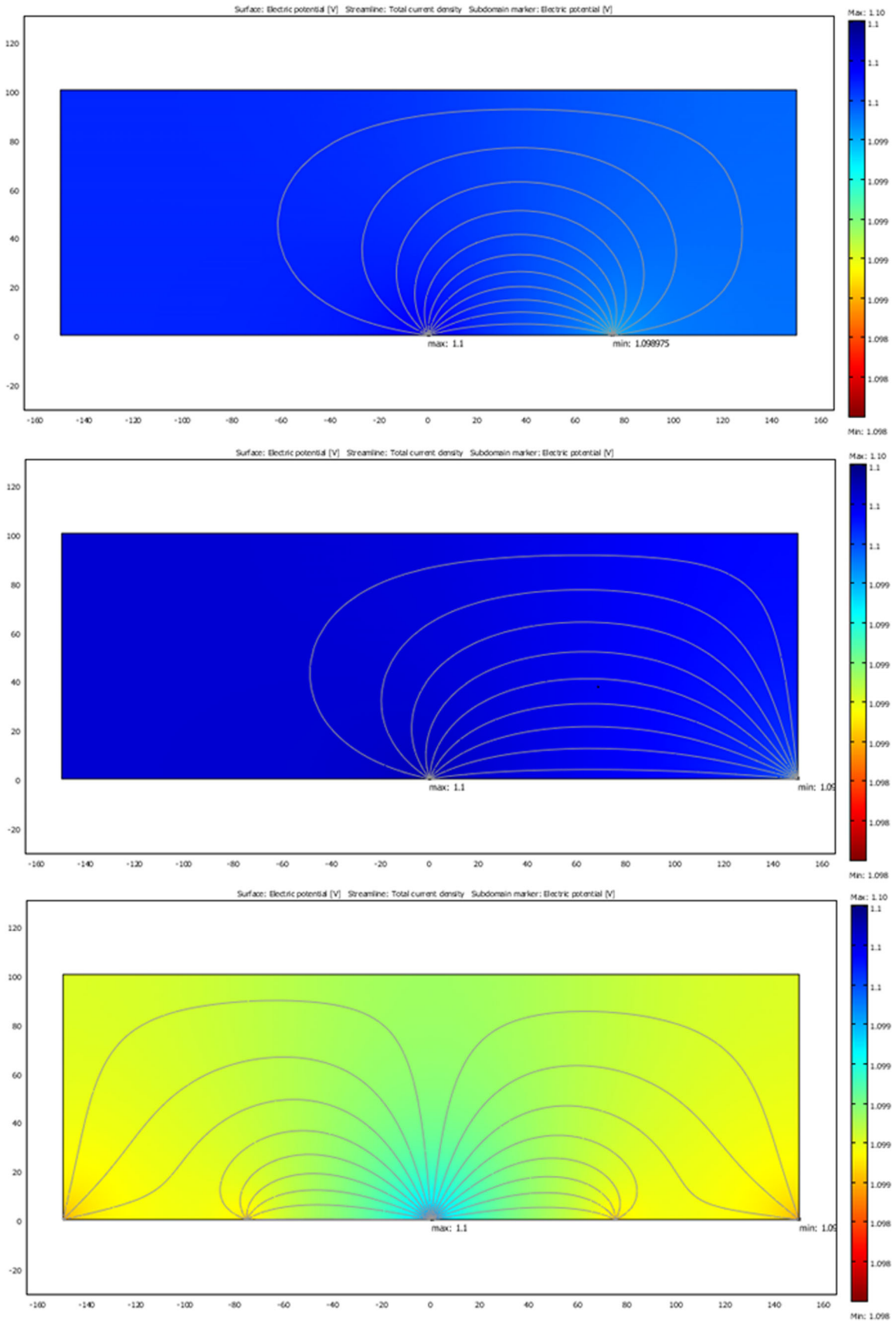

Figure 4. Comparison between FEM modeling of single coating defect (top, center) and four defects (bottom) on a pipeline at 100 m sea depth, defect size 10 mm

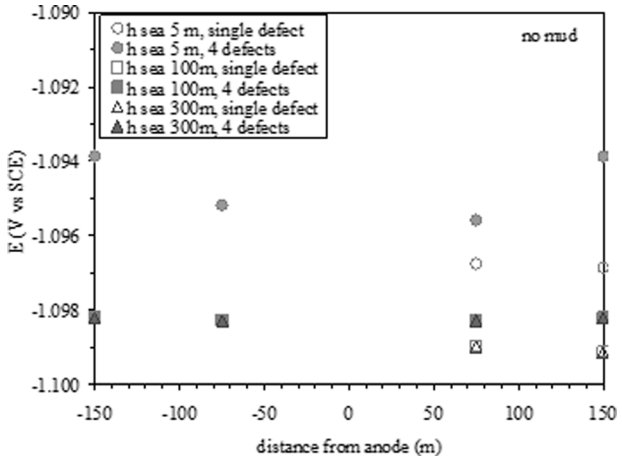

Figure 5. Values of potential in correspondence of four equally spaced coating defects and relevant single defects

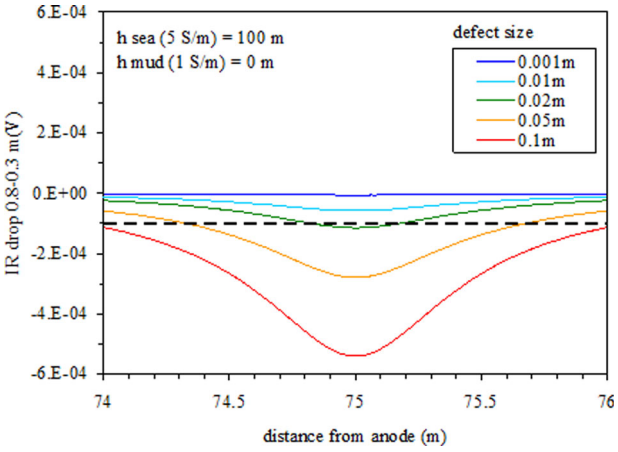

Figure 6. Ohmic drop *versus* distance as a function of coating defects positioned at 75 m from anode (sea depth 100 m, pipeline not buried)

The single defect configuration showed potential values more negative and closer to the anode potential; this effect was evident with low sea depth (5 m) only. The configuration with four defects showed that the potential of defects more distant from the anode was less negative than that of two defects closer to the anode. The results demonstrated that potential distribution on multiple defects cannot be considered as a combination of those obtained with single defects, so that superposition principle is not applicable.

3.2 Potential distribution at coating defects

In this case study, the pipeline is laid on sea bottom, potential-to-defect-size dependence was found to be quite linear, and heavily dependent on sea depth; in an other case study of buried pipeline, a certain deviation from linearity was observed and the influence of sea depth was reduced for a given defect size.

On the basis of FEM results, through ordinary least squares method, the potential can be expressed as a function of defect size and sea depth as shown by the following equations:for $h_m = 0$ (i.e. no burial)

$$E\,[\mathrm{mV}] = -1100 + 0.13 \cdot (w\,[\mathrm{mm}])^{0.9} \cdot (1 + 15 \cdot (h_s\,[\mathrm{m}])^{-1.2}) \quad (4)$$

for $h_m = 0.5$

$$E\,[\mathrm{mV}] = -1100 + 0.29 \cdot (w\,[\mathrm{mm}])^{0.81} \cdot (1 + 5.5 \cdot (h_s\,[\mathrm{m}])^{-1.2}) \quad (5)$$

3.3 Critical defect size detectable by probe

Figure 6 shows, as an example, the variation of the value of $IR_{drop0.3–0.8\,m}$, namely the difference of potential measured by the two reference electrodes positioned at 0.3 and 0.8 m from the surface of the pipeline or from the sea bottom, within 1 m radius range from the defect.

As a general consideration, sea depth equal or higher than 100 m was not an influencing parameter on IR distribution, while sea depths of 5, 10, and 30 m were so; moreover, as the defect size increased, also the peak amplitude increased. Similar trend was observed for laid-on-sea-bottom pipelines *versus* buried pipelines: peak amplitude ($IR_{drop03–0.8\,m}$) increased from laid on to buried pipelines.

In all studied conditions, defects of size of 1 and 10 mm are not detectable during a survey, since the potential gradient, in the proximity of the defect, produces values of $IR_{drop03–0.8\,m}$ below the minimum appreciable one of 0.1 mV.

In case of pipeline laid on sea bottom, the critical detectable defect size is equal to approximately 20 mm, while in the case of burial depth of 0.5 m, the value is approximately 50 mm. Larger size defects are detectable in both conditions.

Figure 7 shows the vertical potential gradient above the defects, clarifying what was observed:

- as the size of the defect increased, the value of the potential at the defect became less negative; a potential gradient more pronounced was observed, particularly in the first few centimeters above the defects;
- in the presence of mud, the potentials were close to the value of −1.1 V *versus* SCE (potential of bracelet galvanic anode), the gradient was higher within the mud layer; the variation of potential was less pronounced than the case of laid-on pipeline;
- the potential trend showed a singular point at the interface mud-water, corresponding to a distortion of the electric field and the current flux lines.

3.4 Effect of burial depth

The effect of burial depth on the ohmic drop detected by two reference electrodes on a probe at a distance of 0.3 and 0.8 m from the surface was evaluated. Burial depth was varied between 0.5 and 2 m, even if rarely exceeds 1 m.

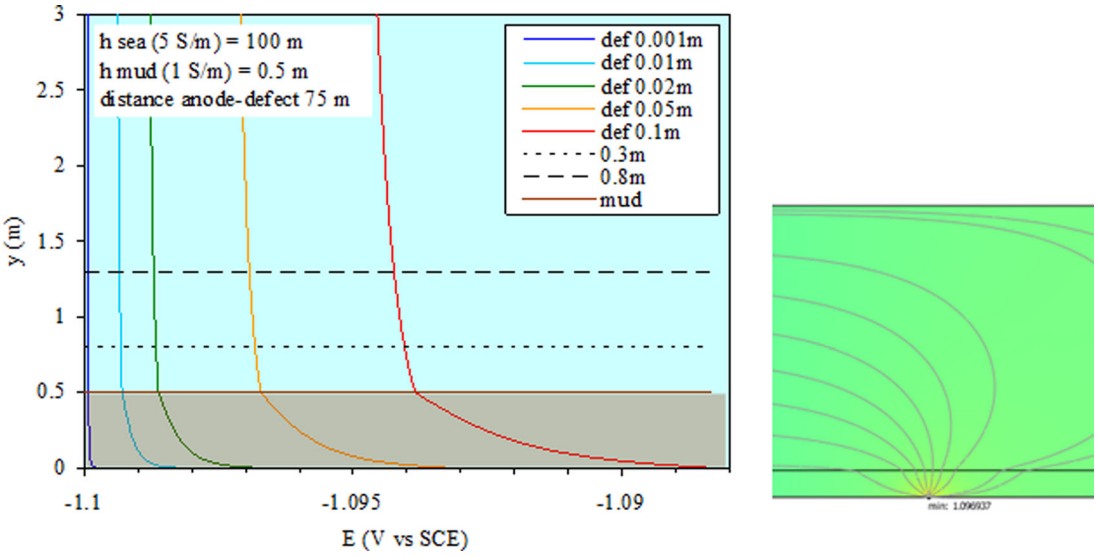

Figure 7. Left: potential gradient as a function of coating defect size, defect positioned at 75 m from the bracelet anode (sea depth 100 m, mud layer thickness 0.5 m); Right: current flow lines near coating defect through the seabed and the sea

By increasing the burial depth, the value of the ohmic drop between 0.3 and 0.8 m decreased and thus the size of the minimum detectable defect increased (Fig. 8).

Linear trends relating the defect size w and the $IR_{drop03–0.8\,m}$ were found. These relationships can be expressed by a single parametric equation, depending on the burial depth and the sea depth:

$$w\,[\mathrm{mm}] = \frac{1000 \cdot \mathrm{IR}_{\mathrm{drop}0.3-0.8\,\mathrm{m}}\,[\mathrm{mV}]}{-5.45 + 4.08 \cdot h_{\mathrm{m}}\,[\mathrm{m}]^{0.22} + f \cdot 4.13 \cdot h_{\mathrm{s}}\,[\mathrm{m}]^{-1.15}} \tag{6}$$

where

$$\begin{cases} f = 0, & (h_{\mathrm{m}} > 0) \\ f = 1, & (h_{\mathrm{m}} = 0) \end{cases}$$

The coefficients of the equation were obtained by least squares method.

This equation assumes that, in the case of presence of mud, the sea depth does not influence the relation between the defect size and the ohmic drop detected between 0.3 and 0.8 m, which only depends on the burial depth. This assumption is in agreement with results obtained by varying h_s and keeping equal to 0.5 m the burial depth, h_m.

On the basis of the results, the relationship between the minimum defect detectable by probe and burial depth can be expressed by the linear equation (Fig. 9):

$$w_{\mathrm{min.detectable}}\,[\mathrm{mm}] = 57.5 \cdot h_{\mathrm{m}}\,[\mathrm{m}] + 17.8 \tag{7}$$

3.5 Example of application of the model to real survey data

Figure 10 shows an example of IR_{drop} data collected during a survey activity in the Red Sea (Egypt) through a probe with two reference electrodes mounted on a ROV.

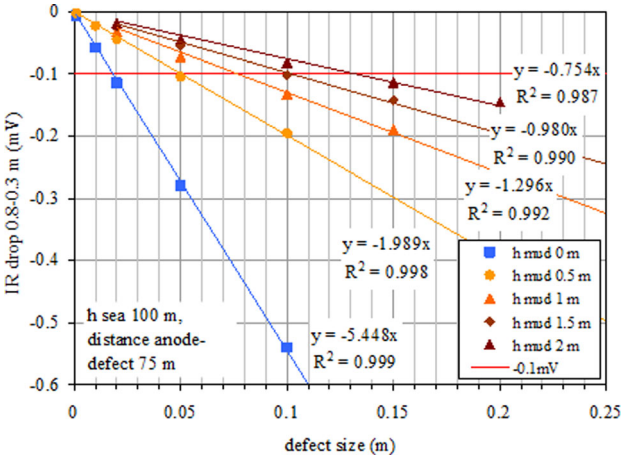

Figure 8. Ohmic drop between 0.8 and 0.3 m distance from the pipeline surface ($h_m \geq 0$) or the seabed ($h_m > 0$), as a function of burial depth

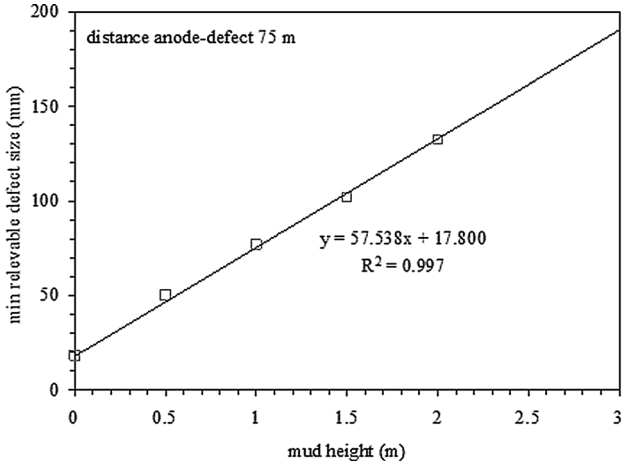

Figure 9. Minimum detectable defect size (mm) as a function of burial depth (m)

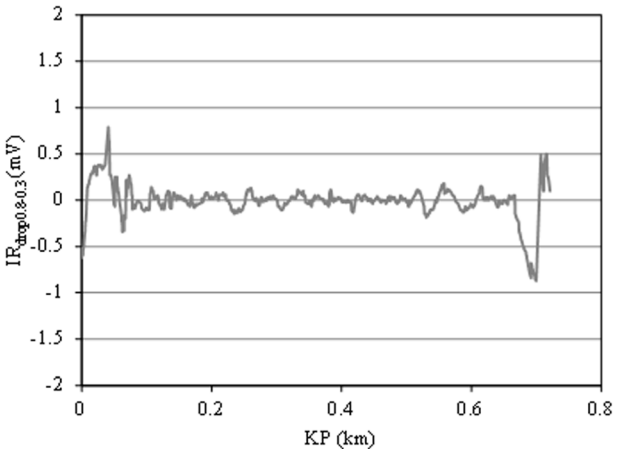

Figure 10. Ohmic drop profile collected during survey activity on an offshore pipeline used as an example for application of the model

In the inspected zone, sea depth was about 16 m and pipeline was laid on sea bottom. Bracelet anode type and dimension are those considered in this paper.

Positive and negative IR_{drop} peaks are respectively related with the anode current output and the current flowing towards steel surface under cathodic protection.

Negative peaks, corresponding to uncoated metal surface, i.e. the cathodic area, can be noticed at Kilometer Point (KP) 0 km and about 0.7 km, with an IR_{drop} value from -0.7 to -0.9 mV.

The profile also shows positive peaks, placed at KP 0.05 and 0.72 km. Positive peaks are commonly detected during survey inspections in correspondence with bracelet galvanic anodes.

The relationship found through FEM analysis can be applied for interpretation of these data. By using Equation (6), for an IR_{drop} value of -0.8 mV, w size of 152 mm is calculated.

This result is compatible with the dimension of uncoated metallic surface of a 10″ pipeline flange. As a matter of fact, flange diameter for a 10″ pipe is about two times the pipe diameter (range is $16'' \div 26''$ as a function of piping class, according to ASME/ANSI 16.5), i.e. 130 mm is the width of the exposed annulus [8]. By considering approximately a flange 20 mm thick, a total dimension of 150 mm for uncoated metallic surface is obtained. As a consequence, uncoated areas were in this case identified with flanges. The following examination of a video taken during ROV survey confirmed the presence of flanges (Fig. 11).

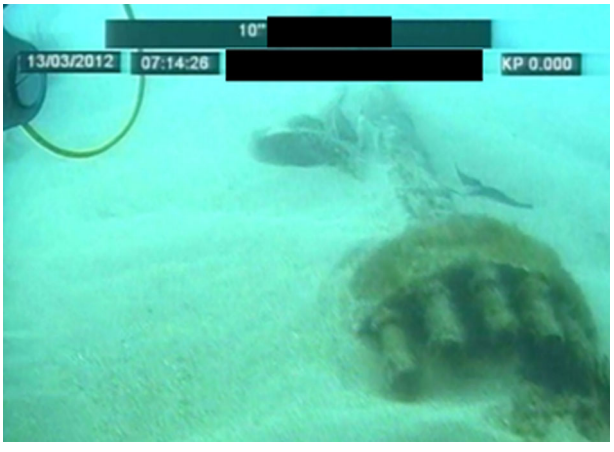

Figure 11. Screenshot from the video taken during survey, at KP 0 km (courtesy of Impresub International LLC, Egypt)

No proper coating defect was detected during this survey. However, results evidenced for flanges can be extended also to defects as the uncoated steel surface behavior is the same from the electrochemical and cathodic protection point of view.

4 Conclusions

A study based on application of FEM modeling was carried out in order to obtain a more accurate interpretation of potential profiles and potential gradient data gathered during survey activities in correspondence with coating damages on offshore pipelines protected with bracelet anodes.

The electrical field near coating defects was modeled by considering a simplified 2D domain and solving, by FEM analysis, the equations given by ohmic drops and overpotentials related to corrosion electrochemical processes on steel surface, i.e. primary and secondary current distributions.

Results showed good consistency with boundary conditions given by the Butler–Volmer equation.

The analysis of four equally spaced defects, compared with that carried out with single defects placed at the same positions, showed that superposition-like principle did not apply.

A good linear correlation between the ohmic drop value measurable by a double reference electrode probe placed above the defect and the defect size was found for each considered geometrical parameter of the domain. Through a parametric equation obtained by interpolation of the coefficients of these linear trends, a relationship between coating defect size and measured ohmic drop, sea depth, and mud burial depth was found.

A relationship between the minimum coating defect size detectable by a double reference electrode probe and the mud burial depth was also obtained.

FEM analysis and the reported parametric equations represent significant and powerful tools for interpretation and better understanding the data collected during an inspection survey.

Acknowledgements: The authors would like to acknowledge Impresub International for the useful cooperation during survey activities in Egypt.

5 References

[1] L. Lazzari, P. Pedeferri, *Cathodic Protection*, Polipress, Milan **2006**.

[2] R. Montoya, O. Rendo'n, J. Genesca, *Mater. Corros.* **2005**, *56*, 404.

[3] R. A. Adey, C. Peratta, J. M. W. Baynham, *NACE CORROSION*, **2012**, Conference Papers, NACE International, Houston **2012**.

[4] F. Liu, S. Wu, *Proceedings of the Twentieth (2010) International Offshore and Polar Engineering Conference*, Beijing, China June 20–25, **2010**.
[5] M. Al-Otaibi, *M.Sc. Thesis*, The University Of British Columbia, Vancouver, November **2010**.
[6] *NORSOK standard M-503*, Edition 3, May **2007**.
[7] S. Lorenzi, B. Bazzoni, P. Marcassoli, T. Pastore, *Corrosion* **2011**, *67*, 026001.
[8] *ASME/ANSI 16.5*, Pipe flanges and flanges fitting, **2009**.